#6791

Journal of Wind Engineering and Industrial Aerodynamics, 35 (1990) 177–200
Elsevier Science Publishers B.V., Amsterdam — Printed in The Netherlands

BOUNDARY TREATMENT FOR THE COMPUTATION OF THREE-DIMENSIONAL WIND FLOW CONDITIONS AROUND A BUILDING

T. STATHOPOULOS and A. BASKARAN
Centre for Building Studies, Concordia University, Montreal, Quebec, H3G 1M8 (Canada)
(Received February 14, 1990)

Summary

This paper addresses the numerical computation of 3-D wind flow conditions around a building. Differential equations are discretized into difference form using the control volume method. Boundary treatment is one of the major issues during the computational process. This paper examines the current boundary treatment methodologies and it proposes a new procedure for boundary treatment with two variables involved in the computation. For most of the cases in which the new method is employed, computed results agree well with the measured wind-tunnel data.

Notation

a_P	hybrid difference scheme coefficient at node P
B	building width
$C_{\bar{p}}$	mean pressure coefficient
$C_\mu, C_2, C_1^1, C_1^{11}$	turbulence model constants: 0.09, 1.92, 2.24, 0.8 respectively
d_P	distance from node P to the solid boundary
D	wall dissipation
E	boundary layer constant: 9.0
G	turbulence generation term
H	building height
k	turbulence kinetic energy
k_P	turbulence kinetic energy at node P
k_e, k_s	turbulence kinetic energy at the edge and within the viscous sub-layer
L	building length
m_ϵ	modified rate of dissipation term
n	streamline co-ordinate
n_P	number of nodes surrounding P
p	fluid pressure
R_c	radius of curvature of streamline

0167-6105/90/$03.50

s	streamline coordinate
S	source term of the differential equation
S_L	linearized source term
S_{ns}	shear strain
U_j	velocity vector
U_P	velocity at node P
U^*	friction velocity
u,v,w	mean velocity components along the x,y,z directions
u',v',w'	fluctuating velocity components along the x,y,z directions
u_s	mean velocity along streamline co-ordinate
U_S	velocity vector with two components
U_g	velocity at gradient height
$\bar{U}_H$	mean velocity at roof height
x,y,z	distances along the coordinate axes
Y^+	normalized wall distance

Greek symbols

Γ_ϕ	diffusion proportionality factor of ϕ
ϵ	dissipation of turbulent kinetic energy
ϵ_s	dissipation of turbulent kinetic energy within the viscous sub-layer
κ	Von Karman constant: 0.4
ν	kinematic viscosity
ν_e	kinematic viscosity at the edge of the viscous sub-layer
ν_t	turbulent viscosity
ρ	air density
σ_k,σ_ϵ	universal constants: 1.0, 1.3
τ	shear stress
ϕ	dependent variable, i.e. u,v,w,k,ϵ

1. Introduction

Building engineers often need information regarding the wind-induced effects on buildings during the design process. This information is available through wind loading standards and codes of practice, which are compiled based on data from various systematic wind-tunnel experiments, sometimes confirmed by full-scale measurements. However, improvements in computer resources offer a new and feasible tool for the evaluation and understanding of wind effects on buildings.

Table 1 taken from Wacker [1], compares the improvements in the computing time for an elliptic boundary value problem. It is clear that the computing time decreases by one to two orders of magnitude within a span of 20 years and it is reasonable to assume that this trend will continue. However, it was only recently that some studies have attempted to simulate the 3-D turbulent wind flow conditions around buildings through computers. This lack of

TABLE 1

Estimated computing time for the elliptic boundary value problem (after Wacker [1])

Year	Dimension	Nodes		
		10	100	1000
1968	1	0.01 s	0.6 s	40 s
(IBM 360-91	2	0.03 s	40 s	10 h
2 MFLOPS)	3	0.6 s	2 h	5 weeks
1987	1	0.0002 s	0.01 s	1 s
(Cray-2 100	2	0.0006 s	0.7 s	12 min
MFLOPS)	3	0.01 s	2 min	15 h

FLOPS is floating point operations per second.

utilization of the booming computer resources by the wind engineering research society is probably due not only to the complexity of the problem but also to the difficulty involved in the numerical modelling of the turbulent process, as explained by Hunt [2].

Vasilic-Melling [3] performed computations for 3-D wind flow conditions around a cube as an extension of her comprehensive work in simulation of 2-D flow over fences. Without including any standard treatment for turbulence, Hanson et al. [4] studied the flow over a building model and their computed results were validated by Summers et al. [5] by using Everett and Lawson's [6] measured data from a boundary layer wind-tunnel. Following a similar procedure to that of ref. 3, Paterson [7] made a systematic effort to evaluate the wind conditions around a building and the wind-induced pressure on the building envelope. His study provides encouragement for further research in this field. To estimate computing time requirements, Baetke [8] studied the wind flow over a cube on a vector computer. Another study which used a supercomputer is described by Murakami et al. [9], who attempted the numerical simulation of unsteady wind conditions by applying the large eddy simulation technique. However, their latter attempts [10,11], to simulate the steady wind conditions around a cubic model used the standard k–ϵ model for the inclusion of turbulence in the computational flow field. Recently the authors [12] computed both the wind velocities around a rectangular building and the wind-generated pressures on the building after modifying the standard k–ϵ turbulence model. The modifications include the streamline curvature correction (Leschziner and Rodi [13]) and the preferential dissipation correction (Hanjalic and Launder [14]). Comparison of the computed results with the measured wind tunnel data indicates significant improvements when the modified turbulence models are utilized.

Studies have also been made using commercially available software. Along

this line, Spalding [15] developed and marketed a general purpose computer code called PHOENICS. Häggkvist et al. [16], Jansson [17] and Richards [18] predicted the wind flow conditions, for different building shapes using PHOENICS. Their results are not always satisfactory when compared with respective experimental data and they generally provide qualitative rather than quantitative agreement.

In numerical modelling processes, boundary specifications for the variables involved play a major role in the computed results. This paper reviews the existing methodologies and suggests a new boundary treatment procedure for two variables involved in the computation of 3-D wind flow conditions around buildings. Comparisons of the computed results made with the measured wind tunnel data indicate that wind velocities, turbulence properties and wind-generated pressures are significantly improved when the new method is applied.

The paper explains briefly the computational methodology, describes the boundary treatment method for the six variables involved (u,v,w,p,k,ϵ) and presents the new boundary treatment method for the turbulent kinetic energy k and its dissipation rate ϵ. Computed results are compared with the measured wind-tunnel data.

2. Computational methodology

This section will outline briefly the computational procedure with more details to be found in ref. 12. In compact form, the necessary differential equations for the 3-D computation of turbulent wind flow conditions around a building can be described by

$$U_j\frac{\partial\phi}{\partial x_j}=\frac{\partial}{\partial x_j}\left(\Gamma_\phi\frac{\partial\phi}{\partial x_j}\right)+S \tag{1}$$

where ϕ is the dependent variable (u,v,w,k,ϵ) and U_j is the velocity vector. The following table provides the values of Γ_ϕ and S for different dependent variables.

ϕ	Γ_ϕ	S	Equation
u,v,w	ν_t	$-\frac{\partial p}{\partial x_i}$	(2),(3),(4)
k	$\frac{\nu_t}{\sigma_k}$	$G-\epsilon$	(5)
ϵ	$\frac{\nu_t}{\sigma_\epsilon}$	$m_\epsilon-C_2\frac{\epsilon^2}{k}$	(6)

and $\nu_t=C_\mu\frac{k^2}{\epsilon}$ (7)

It should be noted that m_ϵ in eqn. (6) is the modified term for the rate of dissipation of k due to the inclusion of dissipation correction and it is calculated using the following expression:

$$m_\epsilon = \frac{\epsilon}{k}\left(C_1^1 G - C_1^{11}\, \nu_t S_{ns}^2\right) \tag{8}$$

In order to include the streamline curvature correction the following expression is used for C_μ, instead of its standard constant value equal to 0.09:

$$C_\mu = \max\left\{0.09,\ 0.09\left[1+0.57\frac{k^2}{\epsilon^2}\left(\frac{\partial u_s}{\partial n}+\frac{U_s}{R_c}\right)\frac{U_s}{R_c}\right]^{-1}\right\} \tag{9}$$

The velocity vector U_s consists of two components, which may be u and v, or u and w, or v and w. The combination which provides the maximum vector has been considered. This is different from the application made in ref. 12, in which only u and v were used to determine U_s. However, no significant difference in the computed results has been found by considering all three velocity components.

In addition to eqns. (2)–(6), the continuity condition has also been included to fulfill the law of conservation of mass. Details for transferring the differential equations ((2)–(6)) and continuity equation into difference form using the control volume method of ref. 19 are reported elsewhere (Paterson [7] and Vasilic-Melling [3]). The final algebraic form of the discretized equation is written

$$a_P \phi_P = \left(\sum_{m=1}^{n_p} a_m \phi_m\right) + S_L \tag{10}$$

in which
P is the grid node where the dependent variable ϕ is computed, n_P is the number of nodes surrounding P, a_P is the hybrid difference scheme coefficient, and S_L is the linearized source term.

The well known SIMPLE algorithm of Patankar [20] is used to correct the velocity field and also to improve the initially assumed pressure field. The advantageous staggered grid arrangement is used. Specification of pressure values on the boundaries is not required by placing the boundaries of the computational domain and the boundaries of the building envelope on the velocity nodes of the staggered grid. Thus boundary treatment is required only for the remaining five variables (u,v,w,k and ϵ), as will be discussed in the following section.

3. Treatment of boundaries

Treatment of boundaries is one of the most important modelling tasks during the numerical evaluation of wind effects on buildings. Figure 1 shows the

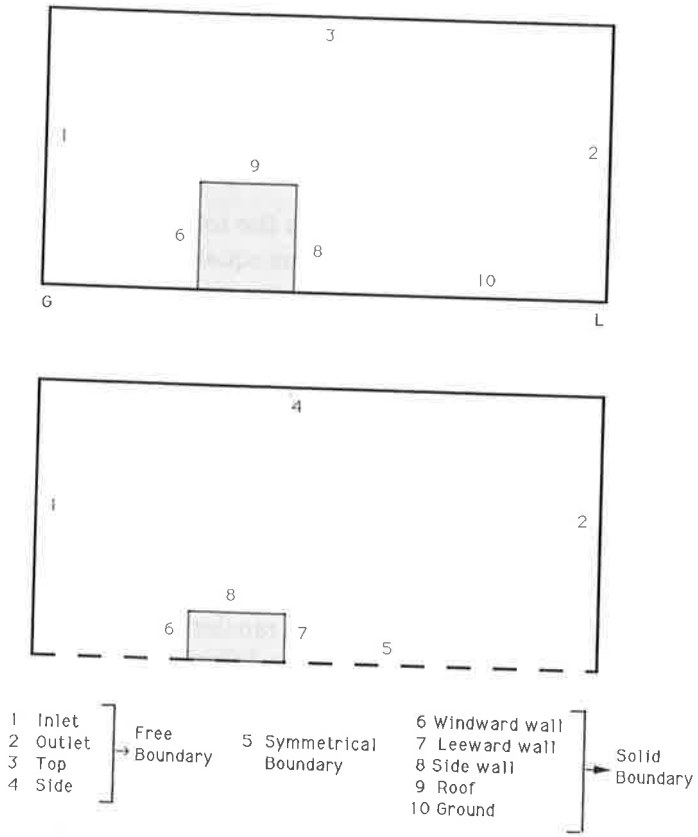

Fig. 1. Boundary locations for 3-D wind flow conditions around a building.

various boundary locations for the calculation of 3-D turbulent wind flow conditions around a building. In total there are ten places where the information of the variables has to be transformed to the computational domain. However, based on their characteristics the boundaries can be grouped under three categories, i.e. free boundaries (1,2,3,4), symmetrical boundaries (5) and solid boundaries (6,7,8,9,10). In most previous studies a common approach is followed for free and symmetrical boundaries whereas differences in treatment are found for solid boundaries.

3.1. Free boundary

Dirichlet boundary conditions are applied for the air-to-air boundaries during the computational procedure. This can easily be done by transforming the values of the variable from IMAX−1 to IMAX, JMAX−1 to JMAX and KMAX−1 to KMAX, if IMAX, JMAX and KMAX are the total number of

grid nodes in the x, y and z directions respectively. A similar exercise is also performed for the values of all variables, on the first node.

3.2. Symmetrical boundary

The normal velocity u and the normal gradient of the other quantities (v,w,k,ϵ) at the axis of symmetry are assumed to have zero value.

3.3. Solid boundary

Researchers follow a variety of approaches for the treatment of different variables in order to identify the presence of the solid boundaries in the computational procedure. For the velocity variables (u,v,w) Vasilic-Melling [3], Murakami and Mochida [10,11] and Baskaran and Stathopoulos [12] use the wall-function approach of Launder and Spalding [21] to bridge the viscous sub-layer (VSL) with the outer region. In accordance with this method, the linearized source term of eqn. (10) is modified based on the wall shear stress $(\tau/\rho)_w$ which can be calculated by the equation

$$\frac{U_P}{(\tau/\rho)_w} C_\mu^{1/4} k_P^{1/2} = \frac{1}{\kappa} \ln\left(E d_P \frac{C_\mu^{1/4} k_P^{1/2}}{\nu} \right) \tag{11}$$

in which U_P is the velocity at node P, k_P is the kinetic energy at node P, d_P is the distance between the node P and the solid boundary, E is the boundary layer constant, approximately equal to 9.0 for smooth wall, κ is the Von Karman constant, and ν is the kinematic viscosity of the fluid.

Equation (11) assumes a region where local production and dissipation of the flow are balanced, shear stress is uniform and the log-law of the wall

$$\frac{U_P}{U^*} = \frac{1}{\kappa} \ln(E Y^+) \tag{12}$$

applies. This is valid for $11.63 < Y^+ < 10^3$, in which Y^+ is the local Reynolds number or normalized (dimensionless) wall distance given by

$$Y^+ = \frac{C_\mu^{1/4} k_P^{1/2}}{\nu} d_P \tag{13}$$

For $0 < Y^+ < 11.63$, a linear velocity profile is appropriate, i.e.

$$\frac{U_P}{U^*} = Y^* \tag{14}$$

Thus the wall shear stress is calculated based on the local flow behaviour and its interaction with the solid surface as well.

For the turbulence kinetic energy k, the turbulence generation term G of eqn. (5) is calculated after Vasilic-Melling [3] by

$$G=\frac{1}{\text{vol}}\int_{\text{vol}}\tau\frac{\partial}{\partial y}(u^2+w^2)^{1/2}\text{d(vol)} \tag{15}$$

in which vol is the boundary control volume.

The rate of dissipation of k for the solid boundary is evaluated by assuming a linear variation of length scale of turbulence with distance from the boundary. With the help of the wall turbulent viscosity, i.e.

$$\nu_t=\kappa U_* d_P \tag{16}$$

and by using the above relation in eqn. (7), the dissipation rate becomes:

$$\epsilon=\frac{C_\mu^{3/4}k^{3/2}}{\kappa d_P} \tag{17}$$

This approach has been followed by Vasilic-Melling [3] and Baskaran and Stathopoulos [12]. It should be noted that Paterson [7] has used a slightly different approach to modify the term S_L in eqn. (10) both for velocity and turbulence variables.

3.4. New Zonal Treatment Method for Solid Boundary

The k–ϵ expressions provided by eqns. (5) and (6) are basically developed for high Reynolds number flows and they are referred to as high Reynolds number turbulent models (HRTM). These are used as engineering tools to simulate only the gross features of turbulence and they do not pay much attention to interactions between the various scales of motion (Bernard [22] and Spalding [23]). Moreover, when the flow is not within the turbulent zone the validity of these equations is questionable. For numerical computation of flows with low Reynolds number and for reproduction of the local laminarization phenomenon, the so-called low Reynolds number turbulent models (LRTM) have been developed by Jones and Launder [24] and Ng and Spalding [25], subsequently modified by Hoffman [26] and Chien [27]. An excellent review of the LRTM used for near wall fluids is presented by Patel et al. [28]. Thus two sets of equations, one for the fully turbulent zones and the other for near wall fluids appear an ideal solution when the wind flow conditions around buildings are considered. However, this approach increases the number of variables to handle and it also demands more computer resources.

In contrast, using eqns. (5) and (6) and modifying the source term of eqn. 10 to account for the presence of the building in the fluid, fails to reproduce the details of the local viscous effect and also creates numerical stiffness problems, see Spalding [23]. Numerical stiffness occurs when the source term is forced to take the full burden of transferring the presence of a building to the computational domain. Moreover, when the grids near the solid boundaries are not fine enough the computed wall shear stress is not realistic and this can

induce numerical divergence during the computational procedure. Naturally, this unwanted situation demands a very dense grid layout near each solid surface which is practically not feasible.

To overcome these problems, a new zonal treatment method is presented for the solid boundary treatment of k and ϵ. In the present approach the HRTM are used only for fully turbulent regions where they are valid. In order to account for the thin VSL near the solid surface, the following procedure is adapted and incorporated into the computer code.

The kinetic energy k for isotropic turbulent motion can be expressed as:

$$k=\tfrac{1}{2}(\overline{u'^2}+\overline{v'^2}+\overline{w'^2}) \tag{18}$$

and by the Taylor series expansion of the fluctuating velocity components near the wall it can be shown (see Jones and Launder [24] and Chien [27] that the kinetic energy of the fluid is approximately proportional to the square of the distance from the solid boundary, i.e.

$$k\propto d_{\mathrm{P}}^2 \tag{19}$$

where d_{P} is the distance of the considered grid node from the solid boundary. One can then obtain the following expression for k within the VSL:

$$k_{\mathrm{s}}=k_{\mathrm{e}}\frac{d_{\mathrm{s}}^2}{d_{\mathrm{e}}^2} \tag{20}$$

in which k_{e} and k_{s} are the kinetic energies at the edge and within the VSL respectively, considered at distances d_{e} and d_{s} from the solid boundary.

The total dissipation rate is not zero near the wall and as explained in refs. 24 and 29, the wall dissipation D is given by the equation

$$D=\nu\left[\left(\frac{\partial\overline{u'^2}}{\partial y}\right)+\left(\frac{\partial\overline{w'^2}}{\partial y}\right)\right]_{y=0} \tag{21}$$

Near the wall, v' the normal component of fluctuating velocity is presumed negligible, therefore, the mean kinetic energy can be deduced from eqn. (18) as:

$$k_{y=0}=\frac{\overline{u'^2}+\overline{w'^2}}{2} \tag{22}$$

Assuming linear variation of the velocity with distance from the wall and combining eqns. (21) and (22), the following relationship is obtained:

$$D=\frac{2\nu k}{y^2} \tag{23}$$

Within the VSL, $D=\epsilon$ and thus the dissipation rate of k can be expressed by

$$\epsilon_s = \frac{2\nu_e k_e}{d_e^2} \tag{24}$$

where ν_e is the fluid viscosity at the edge of the VSL.

The algebraic equations (20) and (24) are used to calculate k and ϵ within the VSL. Equations (15) and (17) are used only for zones outside the VSL. The problem of fixing the edge of the VSL is effectively handled by using the conditions from eqns. (12) and (14).

Even though considerable difficulty exists for the application of the zonal treatment methodology in the computation, its utilization has been found advantageous over the current approach. The new procedure is physically valid and it also alleviates the source term burden in transferring all the information about the presence of solid boundaries into the computational domain. Thus the new approach is not numerically stiff. In addition, improvements are made in the computed values so that better agreement with the experimental data is achieved. This will be discussed in the following sections.

4. Computed results and discussion

In this section the computed results based on the two-boundary treatment methods (zonal treatment and wall functions) are presented. Compared parameters include the kinetic energy (in terms of turbulence intensity of the flow), its rate of dissipation, the pressure and the improved velocity field around the building.

It is generally expected for any computational procedure, that the larger the computational domain and the denser the grid system, the better the computed results. However, the number of computational nodes has a direct influence on the computing time and hence on the cost of computation. The influence of the grid distribution on the computed results was examined by considering the size of the domain and the number of control volumes within the domain. The decision to use a particular grid is made after several grid refinement tests were carried out within the available computer resources.

Figure 2 shows the optimum finite-difference grid layout used in the present study. Both vertical and horizontal sections of the grid layout for a tall building 120 m high, 60 m by 60 m in cross-section are shown. The building in the 3-D computational domain is also presented. The considered layout appears also to be sufficient based on the 2-D experimental study by Antoniou and Bergeles [30] and Bergeles and Athanassiadis [31] and it is consistent with the previous computational works of Paterson [7] and Murakami and Mochida [10]. By using less grid spacing near the solid boundaries and arranging non-uniform spacing for other regions, the efficiency of the present computation increases.

The coordinate system used in the computational procedure is also indicated

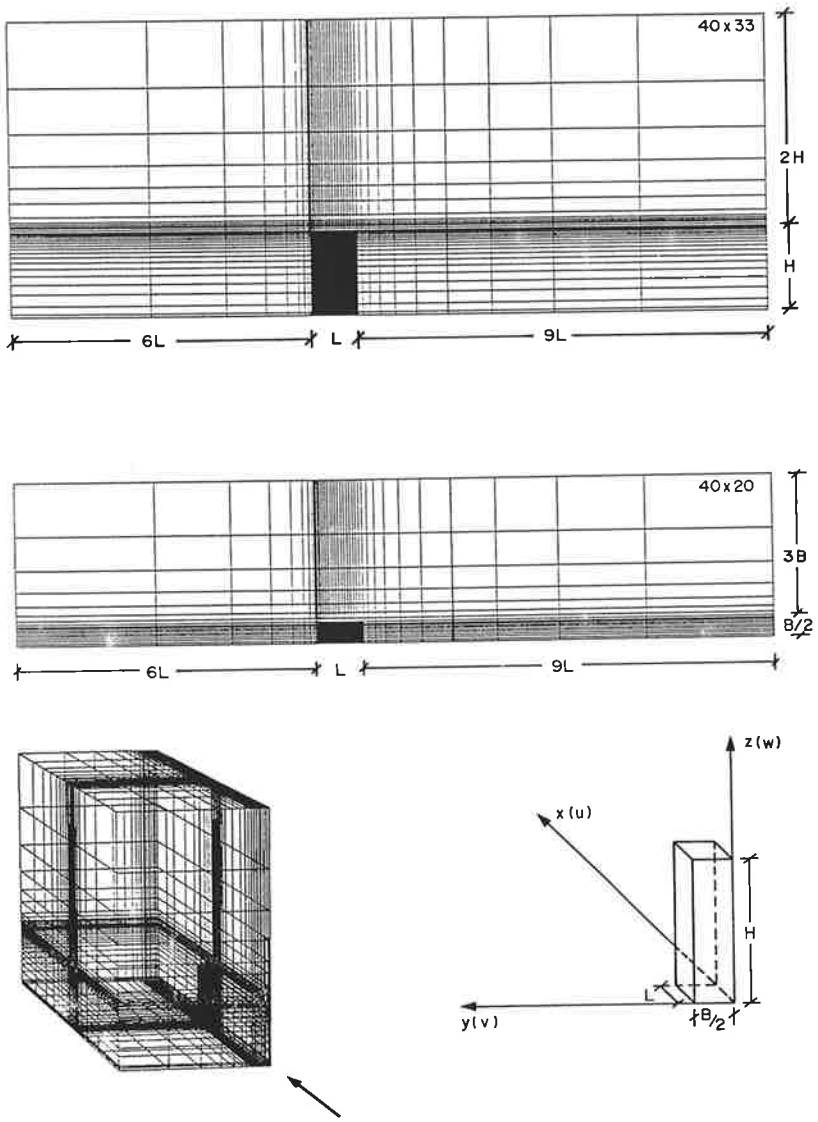

Fig. 2. Computational mesh distributions and co-ordinate system used (only velocity nodes are shown).

in Fig. 2. It should be noted that the x-axis carries the streamwise velocity whereas the lateral and vertical velocities are directed in the y and z directions respectively. All computations have been performed in the Computer Aided Building Design (CABD) laboratory of the Centre for Building Studies by

using the VAX 11/785 (1.2 MIPS) computer. A typical run takes approximately 150 min of CPU time for about 40 iterations.

Figures 3 and 4 present respectively the distribution of turbulence intensity and the rate of energy dissipation around a tall building. The square-root of the computed k values normalized with the free streamwise velocity (at the gradient height) represent turbulence intensity plotted in contour form. Values obtained using the conventional wall function approach and those computed with the new boundary treatment method are compared. It is useful to recall that for the wall function method the source term of eqn. (10) is modified for all five variables (u,v,w,k,ϵ) when solid boundaries are identified during the computational procedure. However, in the new zonal treatment approach only velocity variables are modified based on the local Reynolds number. In contrast, the kinetic energy k and its dissipation rate ϵ are calculated using the

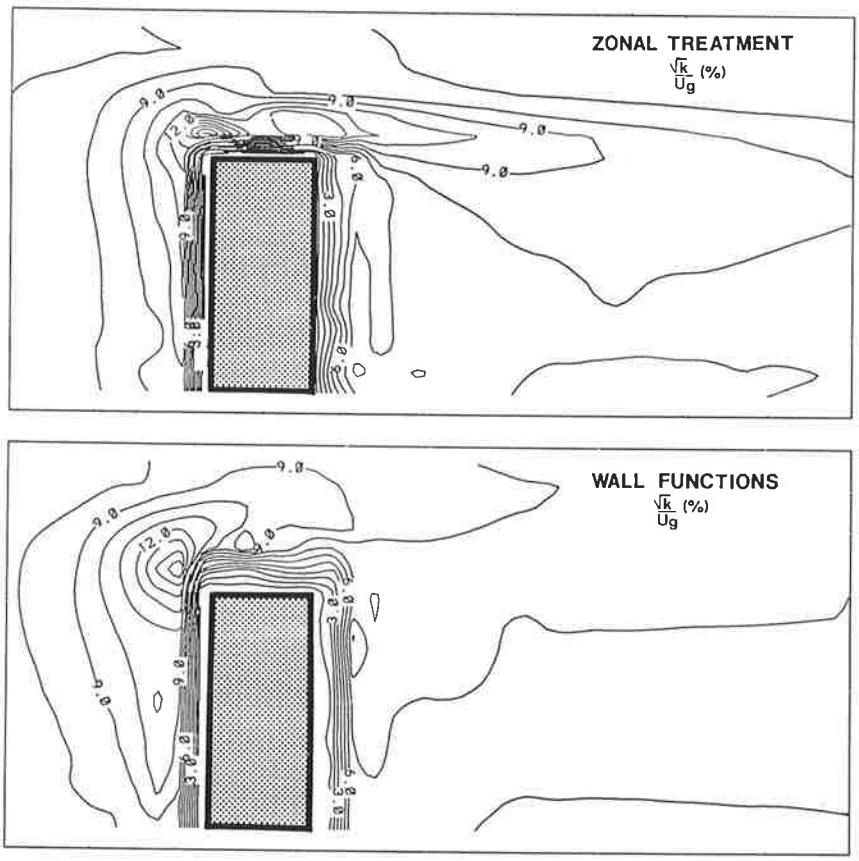

Fig. 3. Computed turbulence intensity around a tall building (side view).

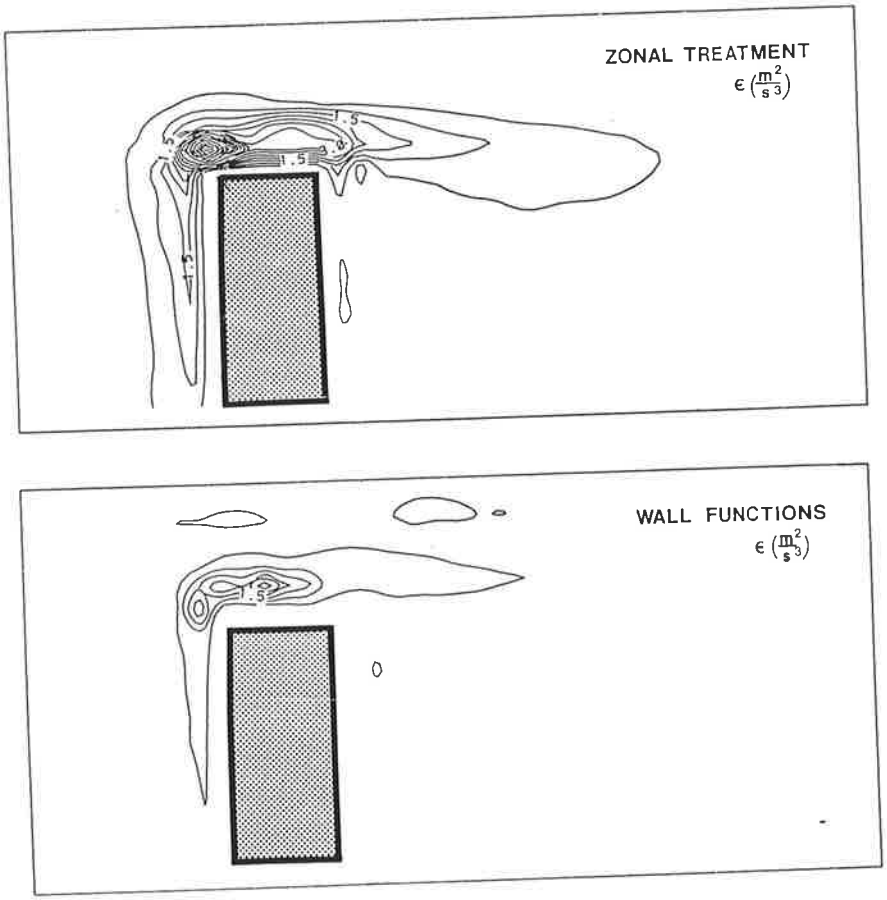

Fig. 4. Computed rate of energy dissipation around a tall building (side view).

algebraic equations (20) and (24) within the VSL whereas for the turbulent zone, discretized equations are modified by using the wall function approach.

In comparing the turbulence intensities obtained by using the two approaches (see Fig. 3) it can be observed that the zonal treatment method provides higher k values near the flow separation region and above the roof surface. In addition, the intensity is also higher in the wake region in comparison with the data obtained by the wall function approach. The peak value of the intensity dies down more slowly in the case of zonal treatment and this is consistent with previous experimental observations discussed in ref. 3. Clearly the VSL representation in the numerical computation provides more accurate results. This can be further noticed in Fig. 4, in which the distribution of dissipation rate of k is presented. Increased k near the solid boundary provides higher ϵ values (see eqn. (24)) and these are found to be more representative

of the actual fluid interaction with the solid surface as explained by Patel et al. [28] and Rodi and Scheuerer [32].

Figure 5 shows the pressure distribution around a building exposed to normal wind conditions, in the format of contour plots similar to Figs. 3 and 4. An increase in positive pressure upstream and constant negative pressure downstream of the building with a zone of zero pressure near separation are evident from the figure. Only marginal differences are found between the two methods for the upstream pressure field. However, differences in the generated negative pressures both on the leeward face and on the roof of the building are clear. The zonal treatment method yields results showing higher suctions on top of the windward portion of the roof and constant suctions maintained further downstream in the wake. This will be further discussed in the comparisons of computed pressure coefficients with respective experimental data.

Velocity vectors and streamline patterns representing the combined influence of the streamwise and vertical velocities are displayed in Figs. 6(a) and

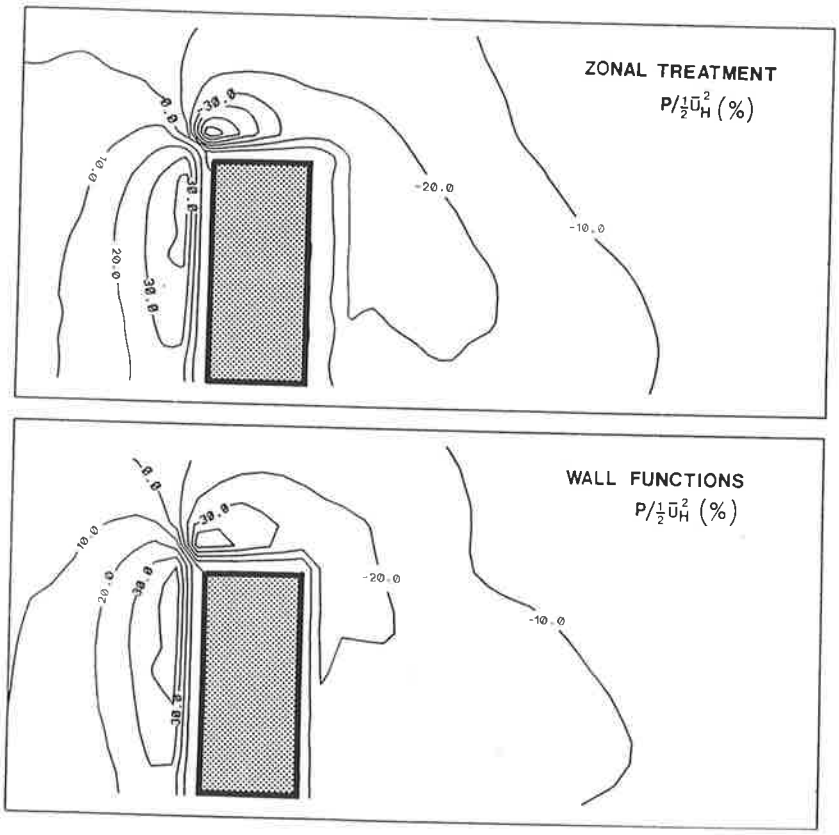

Fig. 5. Computed pressure field around a tall building (side view).

6(b) for a vertical section passing through the centre of the building. The direction of the fluid and its speed locally are shown by the vector plots of Fig. 6(a) whereas the streamlines presented in Fig. 6(b), show the changes in the fluid path relative to the computational domain. Comparing the vectors obtained using the wall function approach and the zonal treatment method, more clear separation from the leading edge and uniform mixing in the recirculation regions are evident when the latter method is used. It should be noted that both plots are obtained by using the same grid distributions. The vector plot based on the wall function approach shows a steep vertical flow behind the building and a strong reverse flow on the roof which do not appear realistic.

Comparing the computed streamline patterns (Fig. 6(b)), the length of the

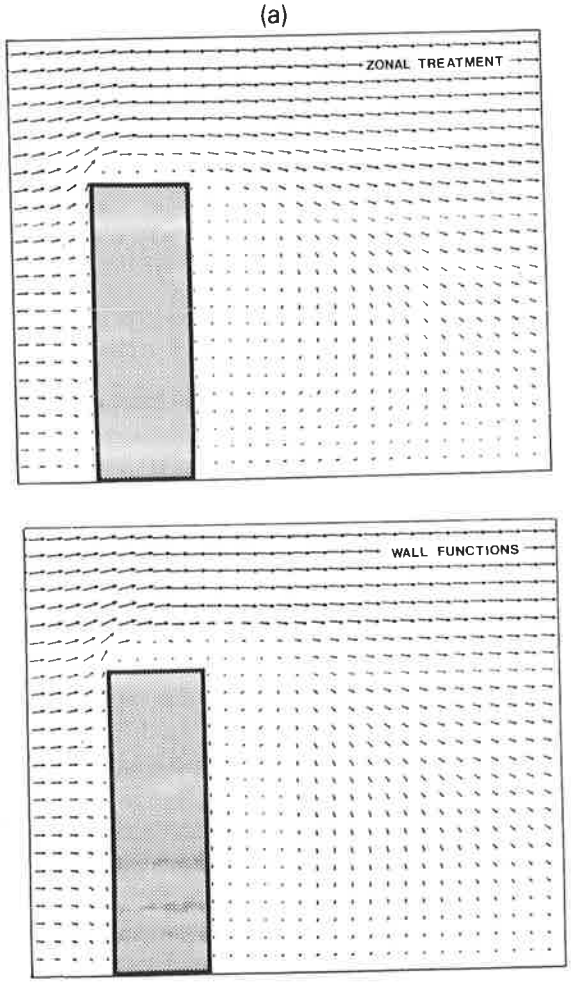

Fig. 6. (a) Comparison of the velocity vectors around a tall building (side view).

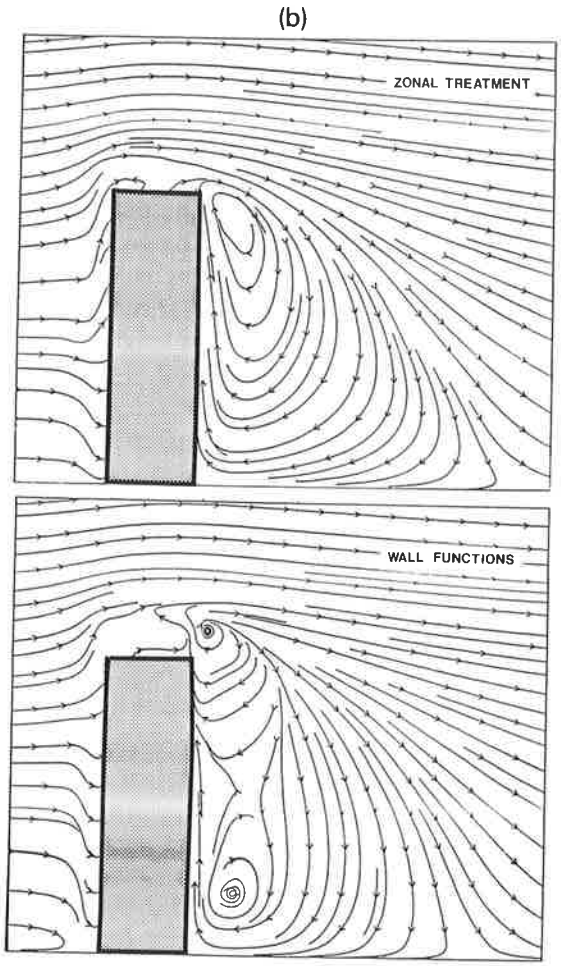

Fig. 6. (b) Comparison of streamline patterns around a tall building (side view).

recirculation zone behind the building is larger and the eddies are more uniformly distributed in the case of the new method. However, the modifications on the standard k–ϵ HRTM relevant to streamline curvature and dissipation corrections are also contributing to these improvements, as reported in ref. 12.

From the above discussion two features become clear. The first is that turbulence properties seem to improve considerably when the new boundary treatment is used. The second feature, which is based on the vector and streamline plots, is that without proper modelling of the local flow conditions unrealistic numerical predictions may be obtained. A more instructive picture emerges when the computed pressure coefficients and turbulence properties are compared with respective measured wind-tunnel data.

5. Comparison of the computed results with measured data

This section presents and compares computed velocities, turbulence intensities and pressure coefficients with respective data obtained from various boundary layer wind-tunnels. Figure 7 shows one such comparison for the stream wise velocity profile. The measured data have been taken from the experimental study of flow over surface mounted cubes by Castro and Robins [33]. Both uniform and turbulent flow conditions were considered in the experiments. However, computations and comparisons are made only for the turbulent boundary layer profile described by a power law exponent equal to 0.25. The vertical velocity profile normalized by the gradient velocity is shown for three different locations. The location $x/L=0.5$ corresponds to the centre of the roof and the other two locations are in the wake of the building. For all three locations the computed results agree reasonably well with the measured wind-tunnel data. The new boundary treatment provides better results in the near wake region $(x/L=1.5)$, whereas both approaches show similar results in other areas.

Figure 8 compares computed and measured turbulence intensities in the same format with Fig. 7. All curves are normalized by the free stream velocity. There are significant differences between measured and computed results in most locations. However, differences also exist between experimental results as well. In order to stress this experimental uncertainty, additional measured data taken

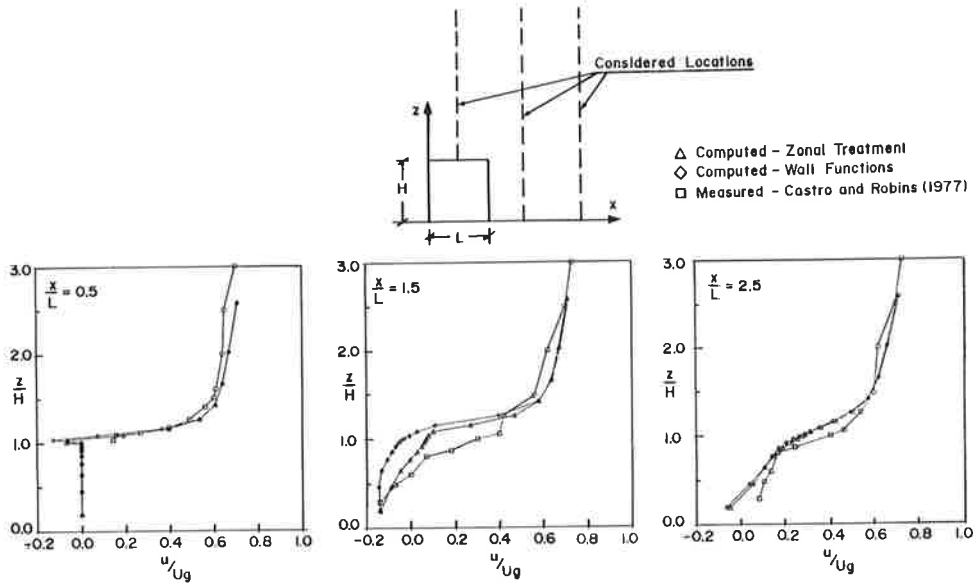

Fig. 7. Comparisons of computed velocity profiles with measured data.

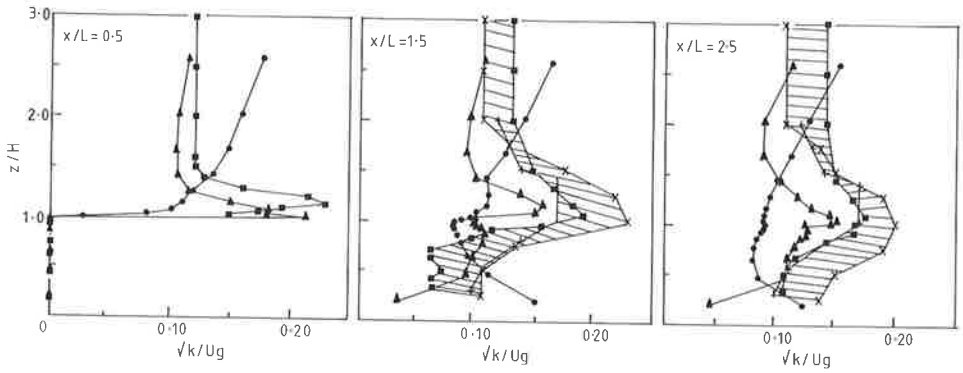

Fig. 8. Comparisons of computed turbulence intensities with measured data.

from Hunt and Smith [34] and Hunt [35] are also included. These correspond to building models of similar dimensions with some variation in the exposure conditions. The range of these experimental data is highlighted in the figure (cross-hatched area). Nevertheless it is quite clear that the data computed using the new zonal treatment approach follow the measured results much closer than those computed by the wall function methodology. This is particularly true of areas near the solid boundary such as right above the roof of the building. Clearly these are the areas in which the considered characteristics of VSL have more influence on the computation.

Figure 9 compares the computed roof pressure coefficient values with the available measured data from two boundary layer wind-tunnel experimental studies, namely Stathopoulos et al. [36] at the University of Western Ontario and Stathopoulos and Luchian [37] at the Centre for Building Studies of Concordia University. Close similarities exist between geometrical and exposure characteristics in both studies. The building models used have a near-cube shape and the exposure simulates open country terrain conditions. The x-axis is normalized by the building length, and the mean pressure coefficients are presented in the vertical axis. Since the building is exposed to normal wind, only half of the roof is considered in the comparison. The four different diagrams in the figure correspond to the variation in pressure coefficients along four locations on the roof. However, experimental data from ref. 37 are available only for $y/L=4\%$.

For all locations the new boundary treatment method yields more satisfactory results as far as the agreement with measured data is concerned. This is justified by the improved turbulence conditions above the roof previously discussed (see Fig. 8). The analysis based on the common wall function approach yields significant underestimations of pressure coefficients on most locations of the roof. However, some overestimation of pressure coefficients produced by the zonal treatment near the windward edge of the roof may not be real

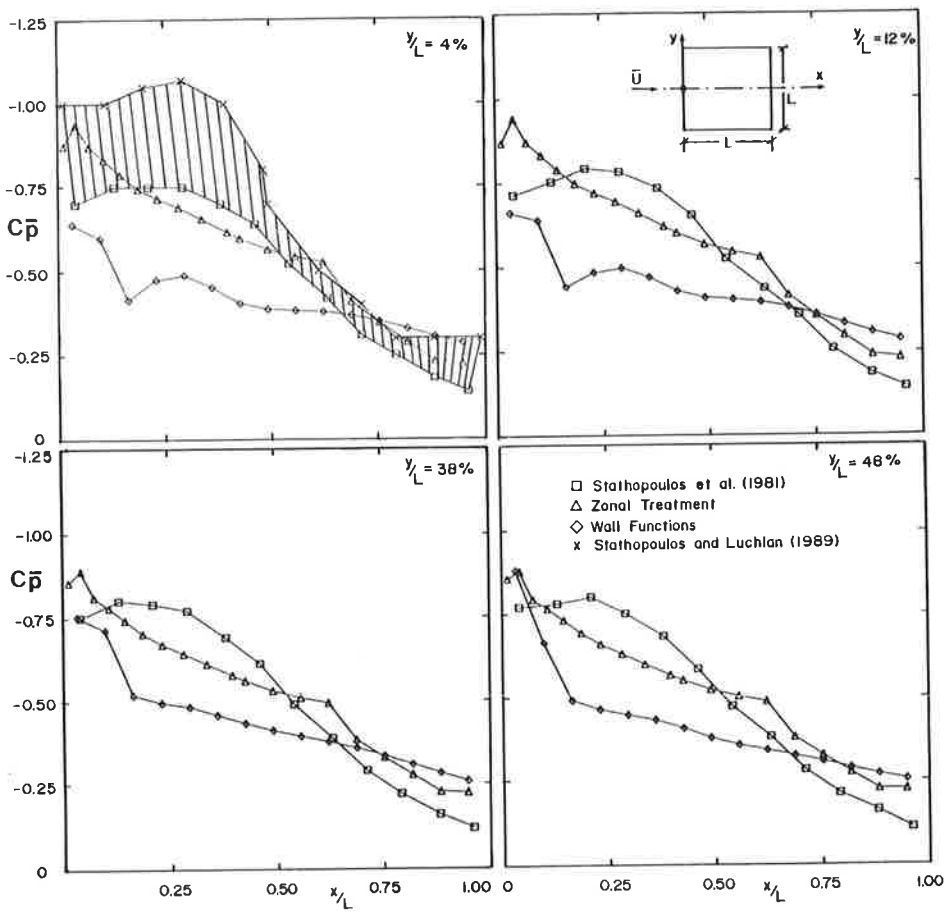

Fig. 9. Computed and measured pressure coefficients on a flat roof.

owing to the variability of the measured data in this region at least for the central roof location, as clearly indicated in the first diagram. It is remarkable that the new method shows much better agreement with the measured data also near the edge of the roof ($y/L=48\%$) where the flow is quite complex in nature.

Comparisons of the pressures on the walls of a 55 m high building with a square cross-section (60 m by 60 m) are shown in Fig. 10. For each wall three curves representing the measured data, the computed values based on the wall function approach and those derived based on the zonal treatment method are depicted. The experimental values are taken from Stathopoulos and Dumitrescu-Brulotte [38]. The values are presented in non-dimensional pressure coefficient form, i.e. pressures normalized by the dynamic velocity pressure

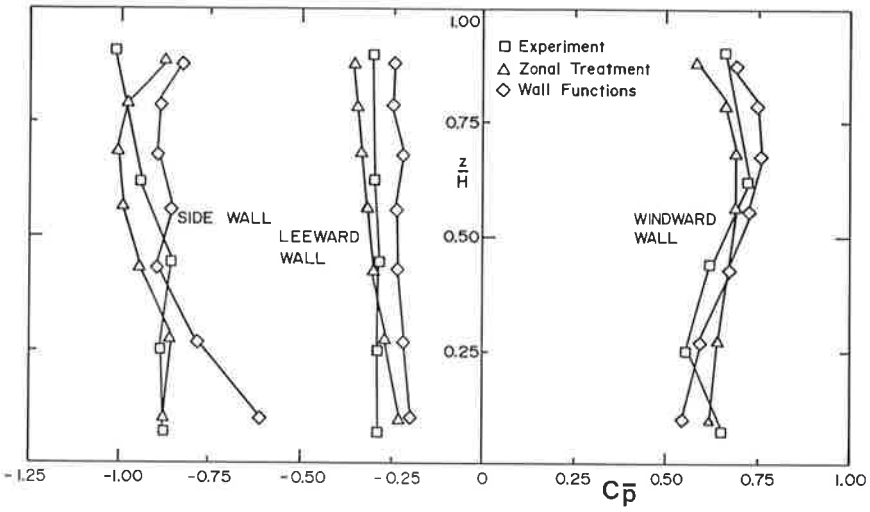

Fig. 10. Computed and measured pressure coefficients on the walls of a building.

measured or computed at the building roof height. Each point in the curve provides the maximum value that has been recorded during the measurements or calculated in the computation at the considered height level of the relevant wall. These values can be directly used for evaluation of external wind-induced pressure loads on the building envelope. These loads are necessary for design purposes. Windward wall positive pressure coefficients and suction coefficients on the side and leeward walls are presented in the x-axis whereas the vertical axis indicates height normalized by the building height. Small difference is found among the three curves in the case of windward wall. However, significant improvement in the leeward wall and better agreement between computed and measured data for the side wall is evident when the new boundary treatment is applied.

In order to validate the zonal treatment method in a general way a more systematic parametric study has been carried out and the results are compared with respective measured data taken from ref. 38. As previously, computations have been performed by using both the wall function approach and the zonal treatment method, for each building configuration and exposure condition. Computed and measured pressures are transformed again into the non-dimensional pressure coefficient form referenced to the dynamic velocity pressure at the respective building roof height. From the pressure coefficients computed or measured, the maximum value that has been found on each horizontal wall section is retained. The arithmetic mean of all these values provides an average critical pressure coefficient for each wall. Thus a single parameter, i.e. the average critical pressure coefficient for each wall, is obtained by deducing large

amounts of available data in order to judge the accuracy of the numerical predictions.

Figure 11 shows comparisons of such average critical pressure coefficients for all walls of a square building ($L/B=1$) with different ratios of H to B. Results computed using the new zonal treatment method are mostly in good agreement with the measured data. Clearly encouraging improvements are obtained for the building side wall irrespective of aspect ratios. For other walls the improvements are also remarkable except when the H to B ratio is too small or too large. Nevertheless, overall the zonal treatment method gives better results in comparison with the wall function approach.

Further investigation will naturally be needed for the application of the suggested new methodology to buildings of different geometries (shapes) and different wind directions. In addition, appropriate experimental data will be required for the purpose of validation. This will be the subject of a future study.

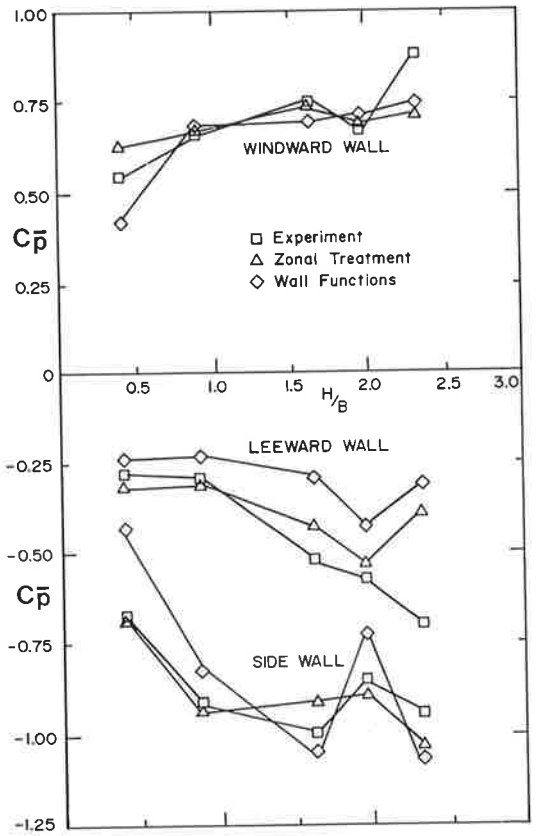

Fig. 11. Computed and measured average pressure coefficients on the walls of buildings with different aspect ratios.

6. Conclusions

A systematic study has been carried out for the 3-D evaluation of wind flow conditions around a building with emphasis on the boundary treatment. Based on the presented results the following conclusions can be made.

(1) Existing wall-function treatment for the kinetic energy and its dissipation rate is not sensitive in predicting the properties of the near-wall VSL regardless of the grid density around the solid boundaries.

(2) The new zonal treatment method attempts to solve the near-wall thin VSL, and hence the fluid turbulence properties (kinetic energy, its dissipation rate and viscosity), are predicted well.

(3) Comparison with the measured wind-tunnel data of the wind velocities and turbulence intensities around buildings, as well as wind-induced pressures on buildings, shows significant improvements, at least for some cases, when the new method is utilized.

References

1 H.M. Wacker, Introduction to the seminar of parallel computing in science and engineering, Proc. 4th Int. German Aerospace Research Establishment Seminar on Foundations of Engineering Sciences, Bonn, June, 1987, pp. 1–11.

2 J.C.R. Hunt, Studying turbulence using direct numerical simulation: 1987 (Centre for turbulence research NASA Ames/Stanford Summer Programme), J. Fluid Mech., 190 (1988) 375–392.

3 D. Vasilic-Melling, Three-dimensional turbulent flow past rectangular bluff-bodies, Ph.D. Thesis, University of London, 1977.

4 T. Hanson, D.M. Summers and C.B. Wilson, A three-dimensional simulation of wind flow around buildings, Int. J. Numerical Method. Fluids, 6 (1986) 113–127.

5 D.M. Summers, T. Hanson and C.B. Wilson, Validation of a computer simulation of wind flow over a building model, J. Build. Environ., 21 (1986) 97–111.

6 T.W. Everett and T.V. Lawson, Wind-tunnel measurements of pressure and velocity around a simple building in a turbulent shear flow to allow validation of values derived from a computer solution of Navier–Stokes equations, Rep. No. TVL/8401, 1984, (Department of Aeronautical Engineering, Bristol University).

7 D.A. Paterson, Computation of wind flows over three-dimensional buildings, Ph.D. Thesis, University of Queensland, St. Lucia, Queensland, 1986.

8 F. Baetke, Numerische Berechnung der turbulenten Umströmung eines kubischen körpers, Ph.D. Thesis, Technische Universität, München, 1986.

9 S. Murakami, A. Mochida and K. Hibi, Three-dimensional numerical simulation of air flow around a cubic model by means of large eddy simulation, J. Wind Eng. Ind. Aerodyn., 25 (1987) 291–305.

10 S. Murakami and A. Mochida, 3-D numerical simulation of airflow around a cubic model by means of the k-ϵ model, J. Wind Eng. Ind. Aerodyn., 31 (1988) 283–303.

11 S. Murakami and A. Mochida, Three-dimensional numerical simulation of turbulent flow around buildings using the k-ϵ turbulence model, J. Build. Environ., 24(1) (1989) 51–64.

12 A. Baskaran and T. Stathopoulos, Computational evaluation of wind effects on buildings, J. Build. Environ., 24(4) (1989) 325–333.

13 M.A. Leschziner and W. Rodi, Calculation of annular and twin parallel jets using various discretization schemes and turbulence model variations, J. Fluids Eng., Trans. ASME, 103 (1981) 352–360.
14 K. Hanjalic and B.E. Launder, Preferential spectral transport by irrotational straining, Turbulent Boundary Layers, ASME, New York, 1979, pp. 101–110.
15 D.B. Spalding, A general purpose computer program for multi-dimensional one and two phase flow, Math. Comput. Simulation, 8 (1981) 267–276.
16 K. Häggkvist, C. Anderson and R. Taesler, PHOENICS – application in building climatology, Lecture Notes in Engineering, Vol. 18, Numerical Simulation of Fluid Flow and Heat/Mass Transfer Processes, Springer Verlag, Berlin 1986.
17 O.B. Jansson, Tryckberäkning Kringsmäklossar, Ser. Anr. 149, 1987 (Water Resources Engineering, Lulea, Sweden).
18 P.J. Richards, Computational modelling of wind flow around low-rise buildings using PHOENICS, DN1508, 1989 (AFRC Inst. of Engr. Research, Silsoe, Bedford, U.K.).
19 L.S. Caretto, R.M. Curry and D.B. Spalding, Two numerical methods for three-dimensional boundary layers, Comput. Methods Appl. Mech. Eng., 1 (1972) 39–57.
20 S.V. Patankar, Numerical Heat Transfer and Fluid Flow, McGraw Hill, New York, 1980.
21 B.E. Launder and D.B. Spalding, The numerical computation of turbulent flows, Comput. Methods Appl. Mech. Eng. 3 (1974) 269–289.
22 S.P. Bernard, Limitations of the near wall k–ϵ turbulence model, AIAA J., 24(4) (1988) 619–622.
23 D.B. Spalding, Turbulence Models, A Lecture Course, Report CFD/82/4, 1982 (Computational Fluid Dynamics Unit, Imperial College of Science and Technology, London, U.K.)
24 W.P. Jones and B.E. Launder, The prediction of laminarization with a two equation model of turbulence, Int. J. Heat Mass Transfer, 15 (1972) 301–314.
25 K.H. Ng and D.B. Spalding, Turbulence model for boundary layers near walls, Phys. Fluids, 15(1) (1972) 20–30.
26 G.H. Hoffman, Improved form of low Reynolds number k–ϵ turbulence model, Physics Fluids, 18(3) (1975) 309–312.
27 K.Y. Chien, Predictions of channel and boundary layer flows with a low Reynolds number turbulence model, J. AIAA, 20(1) (1982) 33–38.
28 V.C. Patel, W. Rodi and G. Scheuerer, Turbulence models for near-wall and low Reynold number flows: a review, J. AIAA, 23(9) (1985) 1308–1319.
29 N.C. Markatos, The Mathematical modelling of turbulent flows, J. Appl. Math. Modelling, 10 (1986) 190–217.
30 J. Antoniou and G. Bergeles, Development of the reattached flow behind surface mounted two-dimensional prisms, J. Fluids Eng., Trans. ASME, 110 (1984) 127–133.
31 G. Bergeles and N. Athanassiadis, The flow past a surface-mounted obstacle, J. Fluids Eng., Trans. ASME, 105 (1983) 461–463.
32 W. Rodi and G. Scheuerer, Scrutinizing the k–ϵ turbulence model under adverse pressure gradient conditions, J. Fluids Eng., Trans. ASME, 108 (1986) 174–179.
33 I.P. Castro and A.G. Robins, The flow around a surface mounted cube in uniform and turbulence streams, J. Fluid Mech., 79(2) (1977) 307–336.
34 J.C.R. Hunt and G.P. Smith, A theory of wakes behind buildings and some provisional experimental results, Note Rd/L/N31/69, 1969 (C.E.G.B. Lab., Central Electricity Research Laboratories, Leatherhead, U.K.).
35 J.C.R. Hunt, Further aspects of the theory of wakes behind buildings and a comparison of the theory with experimental results, Note Rd/L/R1665, 1970 (C.E.G.B. Lab., Central Central Electricity Research Laboratories, Leatherhead, U.K.).
36 T. Stathopoulos, D. Surry and A.G. Davenport, Effective wind loads on flat roofs, J. Struct. Div., ASCE, 107 (1981) 281–298.

37 T. Stathopoulos and H.D. Luchian, Wind pressure on buildings with multi-level roofs, Proc. 6th U.S. National Wind Engineering Conf., Houston, TX, U.S.A., March 8–13, 1989.
38 T. Stathopoulos and M.L. Dumitrescu-Brulotte, Design recommendations for wind loading on buildings of intermediate height, Can. J. Civil Eng., 16 (1989) 910–916.